Acta Crystallographica Section F
Structural Biology and Crystallization Communications
ISSN 1744-3091

Expression, purification, crystallization and preliminary X-ray crystallographic analysis of L-lactate dehydrogenase and its H171C mutant from *Bacillus subtilis*

Yanfeng Zhang*‡§ and Xiaoli Gao§

Genetics Graduate Program, Michigan State University, East Lansing, MI 48824, USA

‡ Current address: Cell Biology and Biochemistry Group, Pacific Northwest National Laboratory, Richland, WA 99352, USA.
§ These authors contributed equally to this work.

Correspondence e-mail: zhangy11@msu.edu

Received 20 October 2011
Accepted 13 November 2011

L-Lactate dehydrogenase (LDH) is an important enzyme involved in the last step of glycolysis that catalyzes the reversible conversion of pyruvate to L-lactate with the simultaneous oxidation of NADH to NAD^+. In this study, wild-type LDH from *Bacillus subtilis* (*Bs*LDH-WT) and the H171C mutant (*Bs*LDH-H171C) were expressed in *Escherichia coli* and purified to near-homogeneity. *Bs*LDH-WT was crystallized in the presence of fructose 1,6-bisphosphate (FBP) and NAD^+ and the crystal diffracted to 2.38 Å resolution. The crystal belonged to space group *P*3, with unit-cell parameters $a = b = 171.04$, $c = 96.27$ Å. *Bs*LDH-H171C was also crystallized as the apoenzyme and in complex with NAD^+, and data sets were collected to 2.20 and 2.49 Å resolution, respectively. Both *Bs*LDH-H171C crystals belonged to space group *P*3, with unit-cell parameters $a = b = 133.41$, $c = 99.34$ Å and $a = b = 133.43$, $c = 99.09$ Å, respectively. Tetramers were observed in the asymmetric units of all three crystals.

1. Introduction

L-Lactate dehydrogenase (LDH; EC 1.1.1.27) is an important enzyme that is involved in anaerobic glycolysis in both prokaryotic and eukaryotic cells. It belongs to the 2-hydroxyacid oxidoreductase protein family and catalyses the last step of the glycolytic pathway, in which pyruvate is reduced to L-lactate concurrently with conversion of NADH to NAD^+. During the reaction, a hydride ion is transferred from the pro-*R* face of NADH to the C2 carbon position of pyruvate (Deng *et al.*, 1994; Burgner & Ray, 1984). LDH is also capable of converting L-lactate to pyruvate. While mammalian LDHs are non-allosteric, most bacterial LDHs are allosteric and require an allosteric factor, fructose 1,6-bisphosphate (FBP), for functional activation (Garvie, 1980). Early studies on the structure of LDH (Grau *et al.*, 1981; Buehner *et al.*, 1982; Abad-Zapatero *et al.*, 1987; Hogrefe *et al.*, 1987; Piontek *et al.*, 1990; Wigley *et al.*, 1992; Iwata & Ohta, 1993; Iwata *et al.*, 1994) revealed that its quaternary structure is highly conserved as a homotetramer. The tetramer shows 222 symmetry through three twofold axis termed *P*, *Q* and *R*. In allosteric LDHs, two FBP molecules bind the LDH tetramer at the *P*-axis interface. Positively charged residues such as arginine and histidine are critical for FBP binding. In particular, the imidazolium rings of histidines from each dimeric subunit are ∼3.5 Å apart and interact with the phosphate groups of FBP. LDH from *Bacillus subtilis* has been suggested to play a key role in fermentative metabolism (Romero *et al.*, 2007). However, detailed structural information that could help in better understanding the functional roles of *Bs*LDH is lacking. In this study, wild-type *Bs*LDH (*Bs*LDH-WT) and a point mutation in which His171 was replaced by a cysteine (*Bs*LDH-H171C) were overexpressed in *Escherichia coli* and purified to near-homogeneity. *Bs*LDH-WT and *Bs*LDH-H171C were crystallized and the crystals diffracted to 2.38 Å (*Bs*LDH-WT with FBP and NAD^+), 2.49 Å (*Bs*LDH-H171C with NAD^+) and 2.20 Å (*Bs*LDH-H171C apo-enzyme) resolution.

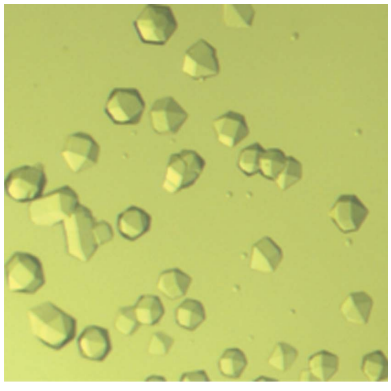

2. Materials and methods

2.1. DNA cloning and site-directed mutagenesis

The DNA encoding *Bs*LDH was amplified from *B. subtilis* genomic cDNA. The PCR amplification consisted of 35 cycles of denaturation at 367 K for 30 s, annealing at 328 K for 45 s and elongation at 345 K for 1 min, followed by 345 K for 10 min. The PCR products were purified using a QIAquick PCR purification kit (Qiagen) and were digested using the restriction enzymes *Nco*I and *Xho*I. The digested product together with pre-cut pLW01 expression vector was transformed into *E. coli* DH5α competent cells. Positive clones grown from LB plates containing 100 µg ml^{-1} ampicillin were picked and plasmid DNAs were isolated and sequenced. Site-directed mutagenesis was performed using the GeneEditor *in vitro* site-directed mutagenesis system (Promega).

2.2. Protein expression and purification

Protein expression was similar to that described previously for other proteins (the receptor-binding domain of botulinum neurotoxins; Zhang *et al.*, 2010, 2011). The sequenced plasmids were transformed into expression host *E. coli* BL21 (DE3) competent cells. A fresh single colony was picked from the selection plate and inoculated into 100 ml LB medium containing 100 µg ml^{-1} ampicillin at 310 K with shaking at 200 rev min^{-1} overnight. 20 ml of this culture was transferred into 1 l fresh LB medium and the cells were grown at 310 K until the OD_{600} reached 0.8–1.0. The cells were then induced by adding 1 m*M* IPTG and incubated at 310 K for 4 h. The cells were harvested by centrifugation and stored at 193 K.

To purify the *Bs*LDH-WT or *Bs*LDH-H171C protein, the cell pellets were resuspended in buffer *A* (50 m*M* sodium phosphate, 300 m*M* NaCl, 0.1 m*M* EDTA pH 8.0). After sonication, the crude cell extract was centrifuged at 277 K for 20 min at 12 000*g*. The supernatant was loaded onto a pre-equilibrated column containing 20 ml Ni–NTA agarose slurry. The column was washed with buffer *A* containing 20 m*M* imidazole. The protein-bound column was eluted with buffer *A* containing 200 m*M* imidazole. The protein eluates were pooled and concentrated to ∼1 ml using an Amicon ultracentrifugal filter (Millipore).

Ion-exchange chromatography was performed to further purify the target proteins. The pooled and concentrated eluates from Ni–NTA affinity purification were loaded onto a 1 ml HiTrap Q ion exchanger (GE Healthcare) pre-equilibrated with buffer *B* (20 m*M* Tris–HCl pH 8.5). Protein was eluted from the column with a linear concentration gradient of NaCl from 0 to 1 *M* at a flow rate of 1 ml min^{-1}. The peak fractions containing highly purified target protein were pooled and concentrated.

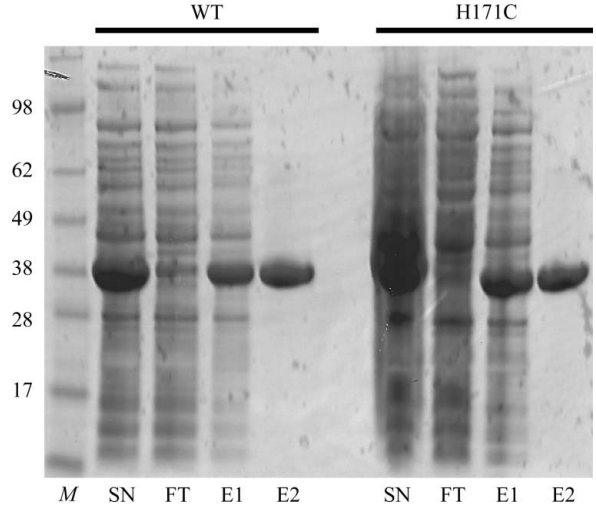

Figure 1
Purification of recombinant *Bs*LDH-WT and *Bs*LDH-H171C. Lane *M*, molecular-weight standard (labeled in kDa); lane SN, supernatant fraction of cell lysate after centrifugation; lane FT, flowthrough fraction from Ni–NTA column; lane E1, eluate from Ni–NTA column; lane E2, eluate from ion-exchange chromatography.

2.3. Crystallization and data collection

Prior to crystallization, the protein concentration was adjusted to ∼10 mg ml^{-1}. 1 m*M* FBP and 1 m*M* NAD$^+$ were added to the protein solution and incubated for ∼1 h before the crystallization trials for obtaining crystals of the complex. Crystals were grown at 293 K using the microbatch-under-oil (1 µl protein solution and 1 µl precipitant) and hanging-drop vapor-diffusion methods (2 µl protein solution and 2 µl reservoir solution equilibrated against 1 ml reservoir solution). For *Bs*LDH-WT, the best crystals grew using a reservoir solution consisting of 16%(*w*/*v*) PEG MME 2000, 0.06 *M* sodium/potassium phosphate, 1.8%(*v*/*v*) glycerol pH 5.5; the best crystals of the *Bs*LDH-H171C mutant were obtained using a reservoir consisting of 14%(*w*/*v*) PEG 4000, 0.1 *M* sodium/potassium phosphate, 2%(*v*/*v*) glycerol pH 7.0. Crystals were transferred stepwise into cryoprotectant solutions with increasing concentrations of glycerol for diffraction studies. 1 m*M* FBP and 1 m*M* NAD$^+$ were included in the cryoprotectant for the crystals of the complex. X-ray diffraction data were collected at 100 K using a MAR CCD detector on the LS-CAT 21-ID-G beamline at the Advanced Photon Source (Argonne, Illinois, USA) with a wavelength of 0.9793 Å. Diffraction data were processed using

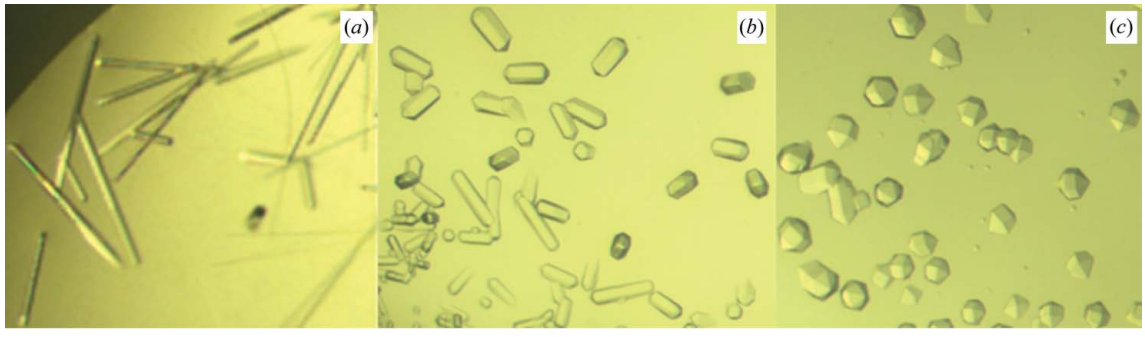

Figure 2
Typical crystals of *Bs*LDH-WT and *Bs*LDH-H171C. (*a*) *Bs*LDH-WT crystals in the presence of FBP and NAD$^+$. The maximum crystal dimensions are about 0.05 × 0.05 × 0.5 mm. (*b*) *Bs*LDH-H171C crystals with FBP and NAD$^+$ added to the protein solution before crystallization trials. The maximum crystal dimensions are about 0.1 × 0.1 × 0.3 mm. (*c*) *Bs*LDH-H171C apoprotein crystals. The maximum crystal dimensions are about 0.2 × 0.2 × 0.3 mm.

Table 1
Data-collection statistics.

Values in parentheses are for the last shell.

Crystals	WT (FBP, NAD^+)	H171C (NAD^+)	H171C (apo)
Space group	*P*3	*P*3	*P*3
Unit-cell parameters			
a (Å)	171.04	133.43	133.41
b (Å)	171.04	133.43	133.41
c (Å)	96.27	99.09	99.34
Data collection			
Detector	MAR CCD 300	MAR CCD 300	MAR CCD 300
Wavelength (Å)	0.9793	0.9793	0.9793
Resolution (Å)	50.0–2.38 (2.47–2.38)	50.0–2.49 (2.59–2.49)	50.0–2.20 (2.28–2.20)
Multiplicity	5.8 (2.7)	5.0 (3.4)	5.4 (4.5)
$\langle I/\sigma(I)\rangle$	15.9 (1.5)	14.4 (3.1)	18.4 (3.7)
Completeness (%)	98.9 (89.9)	99.9 (99.8)	98.9 (99.8)
$R_{\rm merge}$ (%)	8.6 (61.0)	9.5 (40.4)	6.8 (39.9)

DENZO and integrated intensities were scaled using *SCALEPACK* from the *HKL*-2000 program package (Otwinowski & Minor, 1997).

3. Results and discussion

3.1. Protein expression and purification

*Bs*LDH-WT and *Bs*LDH-H171C were expressed in *E. coli* at 310 K for 4 h with a high-level protein yield. The expressed target proteins accounted for ∼50% of the total cell proteins, with >80% in soluble fractions. After Ni–NTA affinity purification, both *Bs*LDH-WT and *Bs*LDH-H171C were further purified by ion-exchange chromatography and eluted at an ionic strength of 0.1–0.15 *M* NaCl (data not shown). Judged by SDS–PAGE, *Bs*LDH-WT and *Bs*LDH-H171C were purified to >95% purity after ion-exchange chromatography (Fig. 1). Approximately 500 mg protein was purified from 1 l *E. coli* cell culture.

3.2. Crystallization and preliminary X-ray data analysis

An initial screen with the microbatch-under-oil method using an Oryx6 crystallization robot yielded crystals from several precipitant conditions. The best crystals (Fig. 2) were produced by further optimization using the hanging-drop vapor-diffusion method.

All three crystals belonged to space group *P*3. The *Bs*LDH-WT crystal diffracted to 2.38 Å resolution and had unit-cell parameters $a = b = 171.04$, $c = 96.27$ Å. The *Bs*LDH-H171C (incubated with FBP and NAD^+) crystal diffracted to 2.49 Å resolution and had unit-cell parameters $a = b = 133.43$, $c = 99.09$ Å. The *Bs*LDH-H171C apoenzyme crystal diffracted to 2.20 Å resolution and had unit-cell parameters $a = b = 133.41$, $c = 99.34$ Å. The X-ray diffraction data-collection statistics for the three crystals are summarized in Table 1. The crystal structure of LDH from *B. stearothermophilus* (PDB entry 2ldb; Piontek *et al.*, 1990) was used for phasing and the molecular-replacement trials gave good solutions. All three protein structures were solved and four monomers were observed in each asymmetric unit. FBP and NAD^+ were observed in the structure of the *Bs*LDH-WT protein, while no ligand was found in the *Bs*LDH-H171C apoprotein structure. Interestingly, NAD^+ was found in the structure of *Bs*LDH-H171C incubated with FBP and NAD^+ but no FBP was observed. The absence of FBP in the structure of *Bs*LDH-H171C (incubated with FBP and NAD^+) indicates that the residue His171 may be critical for FBP binding. Information on the detailed structures will be published later.

This work was performed at the Department of Biochemistry and Molecular Biology, Michigan State University. We would like to thank Dr R. Michael Garavito for helpful guidance and advice on this work and Amy Scharmen for construction of the H171C mutant and technical assistance in purification and crystallization of the wild-type *Bs*LDH protein. Use of the Advanced Photon Source was supported by the US Department of Energy, Office of Science, Office of Basic Energy Sciences under Contract No. DE-AC02-06CH11357. The LS-CAT Sector 21 was supported by the Michigan Economic Development Corporation and the Michigan Technology Tri-Corridor (Grant 085P1000817). We would like to thank Drs David Smith and Spencer Anderson for their assistance in X-ray data collection.

References

Abad-Zapatero, C., Griffith, J. P., Sussman, J. L. & Rossmann, M. G. (1987). *J. Mol. Biol.* **198**, 445–467.
Buehner, M., Hecht, H.-J., Hensel, R. & Mayr, U. (1982). *J. Mol. Biol.* **162**, 819–838.
Burgner, J. W. II & Ray, W. J. Jr (1984). *Biochemistry*, **23**, 3636–3648.
Deng, H., Zheng, J., Clarke, A., Holbrook, J. J., Callender, R. & Burgner, J. W. II (1994). *Biochemistry*, **33**, 2297–2305.
Garvie, E. I. (1980). *Microbiol. Rev.* **44**, 106–139.
Grau, U. M., Trommer, W. E. & Rossmann, M. G. (1981). *J. Mol. Biol.* **151**, 289–307.
Hogrefe, H. H., Griffith, J. P., Rossmann, M. G. & Goldberg, E. (1987). *J. Biol. Chem.* **262**, 13155–13162.
Iwata, S., Kamata, K., Yoshida, S., Minowa, T. & Ohta, T. (1994). *Nature Struct. Biol.* **1**, 176–185.
Iwata, S. & Ohta, T. (1993). *J. Mol. Biol.* **230**, 21–27.
Otwinowski, Z. & Minor, W. (1997). *Methods Enzymol.* **276**, 307–326.
Piontek, K., Chakrabarti, P., Schär, H. P., Rossmann, M. G. & Zuber, H. (1990). *Proteins*, **7**, 74–92.
Romero, S., Merino, E., Bolívar, F., Gosset, G. & Martinez, A. (2007). *Appl. Environ. Microbiol.* **73**, 5190–5198.
Wigley, D. B., Gamblin, S. J., Turkenburg, J. P., Dodson, E. J., Piontek, K., Muirhead, H. & Holbrook, J. J. (1992). *J. Mol. Biol.* **223**, 317–335.
Zhang, Y., Buchko, G. W., Qin, L., Robinson, H. & Varnum, S. M. (2011). *Biochem. Biophys. Res. Commun.* **404**, 407–412.
Zhang, Y., Gao, X., Qin, L., Buchko, G. W., Robinson, H. & Varnum, S. M. (2010). *Acta Cryst.* F**66**, 1610–1613.